Development 140, 1605-1613 (2013) doi:10.1242/dev.088930

Live imaging of multicolor-labeled cells in *Drosophila*

Maria Boulina[1,2], Hasitha Samarajeewa[1,2], James D. Baker[1,2], Michael D. Kim[2,3] and Akira Chiba[1,2,*]

SUMMARY

We describe LOLLIbow, a Brainbow-based live imaging system with applications in developmental biology and neurobiology. The development of an animal, including the environmentally sensitive adaptation of its brain, is thought to proceed through continual orchestration among diverse cell types as they divide, migrate, transform and interact with one another within the body. To facilitate direct visualization of such dynamic morphogenesis by individual cells *in vivo,* we have modified the original Brainbow for *Drosophila* in which live imaging is practical during much of its development. Our system offers permanent fluorescent labels that reveal fine morphological details of individual cells without requiring dissection or fixation of the samples. It also features a non-invasive means to control the timing of stochastic tricolor cell labeling with a light pulse. We demonstrate applicability of the new system in a variety of settings that could benefit from direct imaging of the developing multicellular organism with single-cell resolution.

KEY WORDS: Brainbow, *Drosophila*, Live imaging, Photoactivation, Single-cell resolution, Split Cre

INTRODUCTION

Our knowledge of animal development relies on technologies that are able to reveal detailed cellular events occurring within intact samples. The concept of intactness here is as crucial as it is challenging, however. While the cellular dynamics that would underscore both normal and abnormal development of an animal calls for the highest resolution in analyses, any treatment applied to living cells is likely to be deemed to impact their physiology and morphology, and to trigger an unnatural molecular response within them. In the past, cumbersome experimental procedures were used to examine how individual cells divide, migrate, transform and interact with one another both within and outside the nervous system at different stages of development. One of the most widely employed visualization methods, immunocytochemistry, routinely subjects the samples to fixation and other treatments that can disturb fine cytoarchitecture. Recently, Brainbow, which combines fluorescent proteins and stochastic recombination of gene cassettes, revealed morphological details of individual cells in the mouse brain (Livet et al., 2007). It offered a method that, at least in theory, does not require any pre-treatment before imaging the samples. This innovative multicolor labeling technology also opened the potential to dissect mechanisms that govern the interactions among cells that are either molecularly identical or of the same precursor within the nervous system. Adoption in other model organisms extended Brainbow's use further to include the entire neuronal population, as well as a wide range of non-neuronal cell populations (Hadjieconomou et al., 2011; Hampel et al., 2011; Förster and Luschnig, 2012). However, the current implementations suffer from compromises not only in the controllability and efficiency of the labeling, but also in their compatibility with live imaging. Specifically, *Cre* and *Flp*, the two DNA-editing enzymes adopted successfully, respectively, display low efficiency, i.e. per-cell recombination rate of well under 1%, and little controllability, i.e. virtually ubiquitous and constitutive recombinase activities, in *Drosophila*. Furthermore, none of the model organisms equipped with Brainbow systems so far has pursued live imaging as a preferred approach to visualize the multicolor cell labels. We envisioned that, by refining available tools in *Drosophila*, a model organism that is suitable for live imaging, we would be able to visualize directly the dynamic events that underscore the development of this and other multicellular animals at the level of individual cells. Live imaging, in addition, can dramatically improve data quality by allowing examination of the same samples at multiple time points throughout development. Therefore, we modified the original Brainbow to facilitate cellular visualization within intact *Drosophila*. We added controllability to the DNA editing activities of *Cre* recombinase and, also, prepared stocks that are ready for conducting immediate experiments. LOLLIbow, or live imaging optimized multicolor labeling by light-inducible Brainbow (which is described here), will complement existing genetic tools in *Drosophila* and facilitate the examination of neuronal and non-neuronal morphogenesis of intact animals with single-cell resolution.

MATERIALS AND METHODS

Multicolor cell-labeling Brainbow and light-inducible DNA-editing *Cre* recombinase constructs were each subcloned into a *Drosophila* transformation vector containing the *GAL4* responsive *UAS* site and *PhiC31* integrase recognition sequence, resulting in '*LOLLIbow*' and 'split-*Cre*' stocks, respectively (Fig. 1). Specimens from their cross were subjected to a brief pulse of blue light at a desired time point (Fig. 2). Subsequently, confocal images and movies were collected at embryonic, larval or pupal stage live without dissection.

DNA constructs

Fluorescent proteins

The starting vector Omni was a modified isPIN vector (M.B., S. Deng, S. Celniker, K. Wan and A.C., unpublished; see also www.ispinproject.org). It is a variation of a standard UAS vector that lacks most of the ballast sequences, which helps to increase DNA yield. Omni contains an integration site for *PhiC31*-mediated transformation in *Drosophila*. *Brainbow1.1* construct (Addgene ID 18722) contains *loxN*, *lox2272-1* and *loxP* recombination sites, mKO, mCherry, EYFP and mCerulean sequences, with the last three proteins being targeted to the plasma membrane via

[1]Department of Biology, University of Miami, Coral Gables, FL 33146, USA. [2]Miami Institute of Molecular Imaging and Computation, Coral Gables, FL 33146, USA. [3]Department of Molecular and Cellular Pharmacology, Miller School of Medicine, Miami, FL 33136, USA.

*Author for correspondence (akira.chiba@miami.edu)

Accepted 28 January 2013

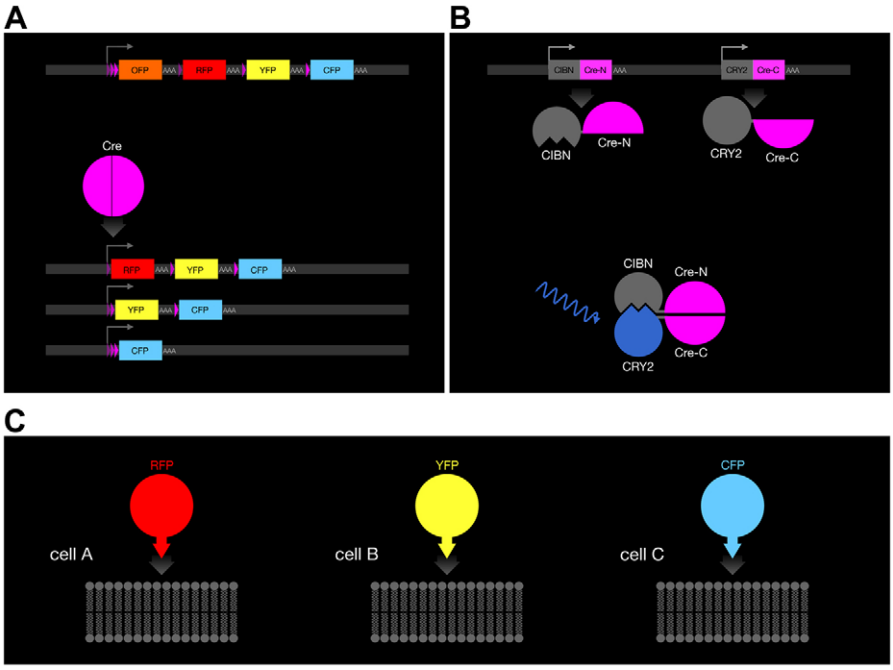

Fig. 1. Molecular design. (**A**) Multicolor cell labeling. 'LOLLIbow' stock contains a *UAS-brainbow* transgene cassette encoding color variants of GFP-like proteins: RFP (mCherry), YFP (EYFP) and CFP (Cerulean) (top). *Cre* recombinase stochastically removes one of the three *lox* cassettes and, subsequently, only RFP, YFP or CFP can be expressed under the control of GAL4 (bottom). (**B**) Photo-inducible *Cre* recombinase. 'split-*Cre*' stock contains *UAS-CIBN::Cre-N* and *UAS-CRY2::Cre-C* transgenes encoding split fragments of *Cre* (top). Blue light induces dimerization of the complementary chimeric proteins (bottom). (**C**) Membrane targeting reveals fine cellular details in each cell with RFP, YFP or CFP (cell A, cell B, cell C).

addition of dual palmitoylation sequence from GAP43 (MLCCIRRTKPVEKNEEADQE). The construct was PCR amplified using PCR suppression strategy (Lukyanov et al., 1996; Luk'ianov et al., 1999) and subcloned into the Omni vector. The construct was sequence verified prior to injecting into *Drosophila*. Transformants were generated using *attP16* and *attP40* integration sites, respectively, on the second chromosome.

Cre recombinase

To generate Split-*Cre* constructs, we essentially used the same vector and strategy. Nuclear targeted CRY::CreN and CIBN::CreC chimerical ORFs (Addgene ID 26888 and 26889) were separately cloned into Omni vector using *Xho*I and *Xba*I cloning sites and the following primers: aaaCTCGAGatgaatggagctataggagg (CIBN_XhoI_DIR), aaaTCTAGA-ctaatcgccatcttccagca (Cre_C_XbaI_REV), aaaCTCGAGatgaagatggac-aaaaagac (CRY2_ XhoI_DIR) and aaaTCTAGAttacagcccggaccgacgat (Cre_N_XbaI_REV). Vectors were integrated using *phiC31* into *attP16* and *attP40* sites on the second chromosome. The construct was sequence verified prior to injecting into *Drosophila*.

Induction of *Cre*

We used a mercury lamp (X-cite 120PC Q 120 W mercury vapor short arc lamp) and a GFP filter (FS 38HE filter configurations: excitation 470/40, dichroic 495, emission 525/50) to induce recombinase activities of the split-*Cre*. Embryos expressing the complementary *Cre* halves received a full field illumination through a 10×/0.30 Air Plan Neofluar objective lens. The illumination pulse of a varied duration consisted of alternating 20 seconds ON followed by 20 seconds OFF (Fig. 2A). It should be noted that samples were exposed to normal room light.

Microscopy

Confocal imaging

Confocal images were taken on a Zeiss 780 inverted confocal microscope with Zen 2010 software, using a 40×/1.3 Oil Plan Neofluar lens. Immersol 518F from Zeiss was used for immersion with the latter. A 25 mW Argon laser was used as the source for the 458 nm (mCerulean), 488 nm (EYFP) and 514 nm (Kusabira Orange) excitation and a 20 mW DPSS laser for the 561 nm (mCherry) excitation. Laser powers of 9.0%, 3.5%, 1.2% and 1.2% with spectral detection ranges of 463-500 nm, 498-515 nm, 550-568 nm and 625-669 nm, respectively, were used as acquisition settings with a pixel dwell time of 50.4 µseconds. Where appropriate, tiling and digital zooming were applied. No spectral unmixing was employed to distinguish the multicolor labels.

Movies

Morphologically staged pupae were selected for imaging and studied using the same Zeiss confocal microscope or a Leica SP5 laser-scanning confocal microscope. Settings for the latter were adjusted to minimize exposure time and laser intensity while still capturing high quality images: CFP and YFP were detected with an Argon laser with 5 mW 458 nm (mCerulean) set to 31% and 5 mW 514 nm (EYFP) set to 7%. RFP was detected with a 20 mW DPSS laser (mCherry) set to 9%. Dwell time was minimized by using the resonance scanner at 8000 Hz. Data consist of *z* series through the 10-15 µm epithelium, collected over time. The movie of a crawling first instar larva, on the other hand, used a spinning disc confocal microscope with a 10×/0.30 Plan Neofluar lens. This system consisted of a Yokogawa CSU X1 spinning disk unit, equipped with continuous wave lasers, dichroic filter sets (Semrock Di01-T 405/488/568/647 beam splitter with 483/32 and 542/27 emission filters for 488 nm and 561 nm lasers, respectively) and an EM-CCD camera (Photometrics Quant EM 512SC) mounted on an inverted Zeiss AxioObserver fluorescent microscope (Intelligent Imaging and Innovation). Exposure time for each channel was 500 mseconds. All movies were imaged at room temperature.

Live imaging

Before imaging the live embryos, we removed the chorion membrane chemically with 50% bleach solution exposure for three minutes at room temperature. Embryos were transferred onto a large 40×22 mm coverslip (No 1.5 from Corning or VWR), covered with halocarbon oil (Halocarbon Products, CAS#9002-83-9), and mounted on the inverted microscope. For imaging the live larvae, their cuticle skin was washed thoroughly with water. Except for taking movies to capture the locomotion of the sample (see supplementary material Movies 1, 2), we used an extra coverslip (18×18 mm or 22×22 mm number 1 or 1.5) over the vacuum grease spacer and with some manually applied pressure to minimize their movement during the imaging session. The sufficient pressure was individually checked carefully in each case though visual inspection, while the total imaging duration was kept minimal at 5-20 seconds per 512×512 pixel slice. Pupae were each washed and mounted in a glass-bottomed 25 mm Petri dish (WillCo-Dish). A layer of thiodiethylene glycol between the pupal case and the coverslip reduced refraction. Following the imaging session, samples were each collected with a soft brush and transferred onto yeast-agar plates.

Drosophila stocks

The following homozygous stocks are available upon request: *UAS-CIBN::Cre-N,UAS-CRY2::Cre-C* (*UAS-CIBN::Cre-N* at attP16 and

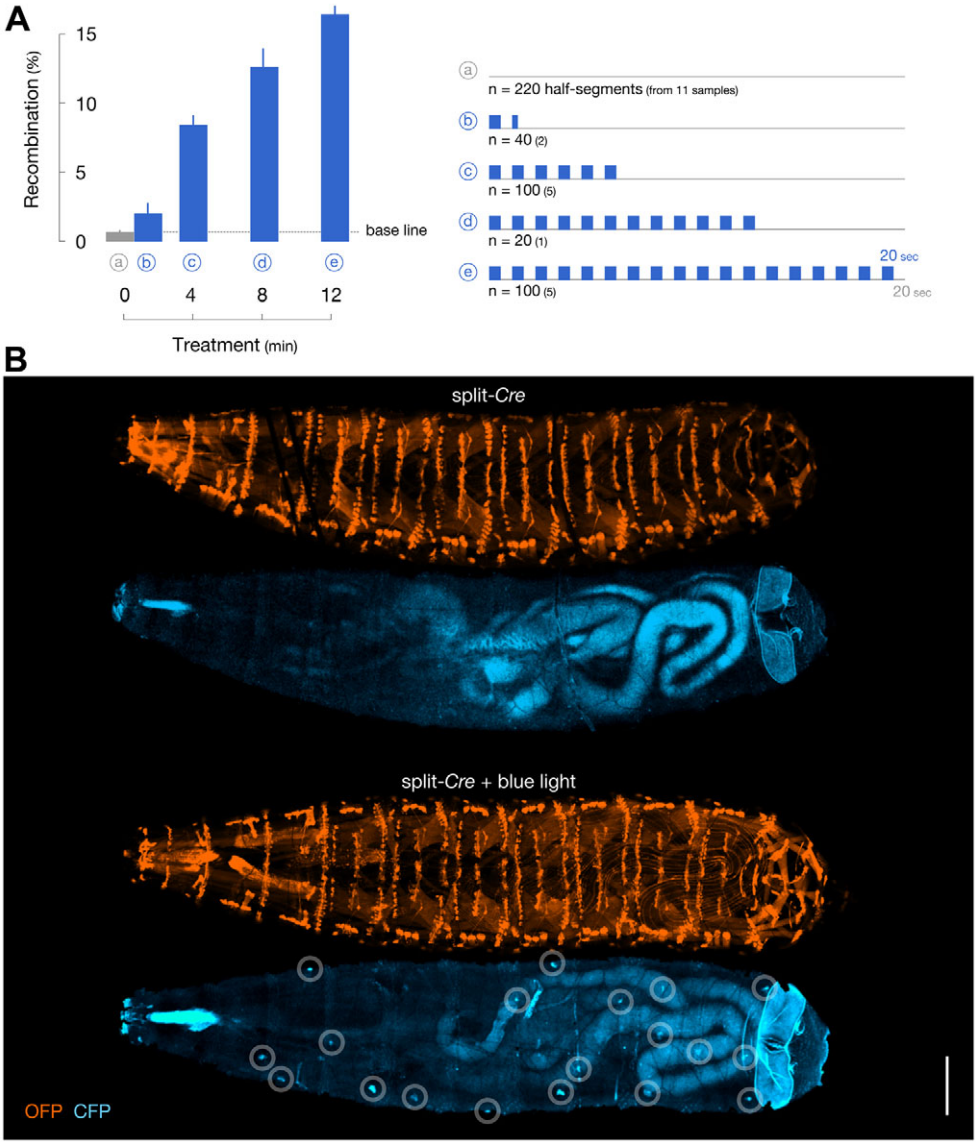

Fig. 2. Light-inducible labeling. (**A**) Per-cell DNA recombination rate is determined by counting the number of CFP-positive cells 48 hours after blue light illumination of 0-, 0.5-, 4-, 8- and 12-minute pulse durations. The baseline is below 1%. (**B**) Tendon cells in larvae visualized using the *GAL4*^{24B} driver: with split-*Cre* but no illumination (top), and with split-*Cre* after a blue light illumination (bottom). Images used two channels, one to show the default label (OFP) and the other to show the recombined label (CFP). Circles indicate the CFP-positive tendon cells. The skeletal muscle cells express fluorescent proteins under the *GAL4*^{24B} at low levels. Gut, esophagus and cuticle display autofluorescence. Scale bar: 50 µm.

UAS-CRY2::Cre-C at *attP40* on the second chromosome), *UAS-brainbow;elav-GAL4* (*UAS-brainbow* at *attP16* on the second chromosome and *elav-GAL4* on the third chromosome), *UAS-brainbow*^{2X} (*UAS-brainbow* at both *attP16* and *attP40* on the second chromosome), *UAS-brainbow*^{2R} (*UAS-brainbow* at *attP16* on the second chromosome) and *UAS-brainbow*^{2L} (*UAS-brainbow* at *attP40* on the second chromosome). The last two may be used to create additional '*LOLLIbow*' stocks for subpopulations of neurons or various non-neuronal populations. *hs'-Cre* lines #766, #851 and #1092, used in this project for comparison with the light-inducible split-*Cre* and *elav-GAL4* line #8760 were obtained from the Bloomington Stock Center.

RESULTS

We combined a Brainbow gene cassette encoding tricolor fluorescent proteins (Livet et al., 2007) to photo-inducible split-*Cre* recombinase (Kennedy et al., 2010) for use in *Drosophila* (Fig. 1). To visualize morphological details of individual cells *in vivo* without relying on immunological signal amplification, we chose a cassette that renders each cell to inherit a permanent assignment among three membrane-targeted GFP-like fluorescent proteins. To control the DNA recombination events, we adapted the light-activated split *Cre* as a non-invasive approach. To facilitate examination of the neurons, we prepared two stocks: *UAS-CIBN::Cre-N,UAS-CRY2::Cre-C* (the 'split-*Cre*' stock) and *UAS-brainbow;elav-GAL4* (the pan-neuronal '*LOLLIbow*' stock) (see below for examining non-neuronal cell populations using other *GAL4* drivers). Our new system is simple to use in a variety of neurobiology and developmental biology experiments: (1) collect samples from the genetic cross between 'split-*Cre*' and '*LOLLIbow*' stocks; (2) illuminate the samples with blue light at a desired time point; and (3) examine the samples live. Depending on one's choice of a '*LOLLIbow*' stock, a defined population of neurons and/or non-neuronal cells are labeled individually with distinct colors.

Effective recombination

In *Drosophila*, both *Flp* and *Cre* recombinases have been successfully adopted to Brainbow systems (Hadjieconomou et al., 2011; Hampel et al., 2011; Förster and Luschnig, 2012). Although the two DNA-editing mechanisms of *Saccharomyces cerevisiae* and P1 bacteriophage origins, respectively, work similarly in many respects, they pose nearly opposite issues in practice. On the one hand, *Flp*, which is used in Flybow (Hadjieconomou et al., 2011), is able to recombine Brainbow cassettes at low efficiencies with its

estimated per-cell recombination rate of well below 1%. Meanwhile, *Flp* causes no apparent toxicity and its variant *mFlp5* further allows for simultaneous use of Brainbow and MARCM (Lee and Luo, 1999) systems in the same animal. On the other hand, *Cre*, which is used in separate *Drosophila* Brainbow systems (Hampel et al., 2011; Förster and Luschnig, 2012), exhibits much higher per-cell recombination efficiency than does *Flp*. However, available *Cre* lines under the control of a heat shock promoter lack consistency in when and where its DNA editing might take place within the animal. As a result, an unknown number of cells in a given cell lineage can inherit a single color, often defeating the purpose of labeling individual cells with multiple colors. Furthermore, as its continual activities can be toxic to the animals (Siegal and Hartl, 1996; Heidmann and Lehner, 2001), studies using a continuous promoter, such as *hs'-Cre*, should proceed with caution.

Many multidomain enzymes that are useful in molecular biology, such as *GAL4*, have been modified to allow artificial control over their *in vivo* activities by splitting them into two moieties. In 2010, a system was reported in cell cultures in which *Cre* activities were engineered to be induced by light (Kennedy et al., 2010). Two complementary fragments of *Cre* recombinase were each chimerized to two plant proteins that are capable of dimerization in a light-dependent manner. To create photo-inducible split-*Cre*, the N-terminal fragment of the recombinase was fused to cryptochrome 2 (CRY2) and the C-terminal fragment to a truncated version of CIB1 (CIBN). Both plant proteins carry nuclear localization tags for efficient assembly. We implemented this system in *Drosophila* for high-fidelity control of *Cre*-mediated DNA recombination (Fig. 1B). Each half of the *Cre* recombinase was cloned into a vector containing five repeats of upstream activation sequence (UAS) in place of the mammalian promoter used in the original study. Our transformation vector also contained an *attB* site that enables targeted landing of the construct at a chosen locus in the *Drosophila* genome. The two parts can be recombined in a single fly line (see below). Using this, we co-expressed both halves of split-*Cre* within the same cells in embryos under the control of a *GAL4* driver. By further illuminating the embryos with blue light, we activated photo-inducible split-*Cre*. To calibrate the photo-induction protocol, we chose to focus on the tendon cells (Volk, 1999). These uni-nucleated cells occur throughout the epidermis of the embryos/larvae as discrete patches at well-known locations in all segments. Although their lineage is not fully described, the tendon cells will have completed their last round of cell division and reached their stereotyped positions by hour 12 of embryogenesis. We used the $GAL4^{24B}$ to drive both *UAS-CIBN::Cre-N,UAS-CRY2::Cre-C* and *UAS-brainbow* in these cells. Their expression begins prior to hour 12. From hour 12 onwards, however, the tendon cells maintain a high-level expression through the end of larvogenesis, or for the duration of ~3.5 days at 25°C. Our goal was to determine the protocol that would: (1) use a simple illumination device; (2) not compromise the survival of the animal both during and after the treatment; (3) complete the induction of recombination within a single cell cycle period, i.e. in as little as 9 minutes in embryos; and (4) attain a sufficiently high per-cell recombination rate of multicolor cell labeling. We subjected the embryos to a mercury lamp with a GFP filter through a 10× air objective lens. The baseline recombination rate, i.e. without the blue light illumination as described below, was below 1%. Prior to treatment, the embryos were de-chorionated to facilitate light penetrance and were covered with halocarbon oil to avoid dehydration. The embryos at hour 12 of their embryo development were then hand picked and placed on a coverslip in random orientations. On a microscope, we applied the blue light as a brief pulse of alternating illumination, with 20 seconds on followed by 20 seconds off, lasting anything up to 12 minutes of a total treatment period (Fig. 2). After the treatment, we transferred the embryos to a small agar-yeast dish. Following 48 hours of subsequent incubation at 25°C, we examined the experimental animals, which by then had reached their second instar larval stage, using confocal microscopy. We imaged each animal twice from two opposite directions. The total number of the tendon cells in view was counted using the OFP channel (514 nm excitation, 550-568 nm detection), the default fluorescence in all GAL4-positive cells. Using the CFP channel (458 nm excitation, 463-500 detection), we determined the number of tendon cells that expressed CFP. Assuming an equal probability for inheriting each of the tricolor choices of the LOLLIbow, however, we estimated the per-cell recombination efficiency by multiplying the number for CFP-positive cells by three. Each of 24 samples offered 20 thoracic and abdominal half-segments and, on average, 380 tendon cells were scored in each sample with a total of over 9000. Statistically significant recombination ($P<0.01$ with two-tailed *t*-test) occurred after illumination for as little as 30 seconds, or 1 minute of treatment in total. However, 12 minutes of treatment, the longest we tried, resulted in an average of 15% per-cell recombination efficiency. In our experiments, the survival rate was close to 90% for both illuminated and non-illuminated samples, indicating that their viability is not compromised. Based on this test, we predict that a short (8-12 minutes) illumination with a blue light pulse would be capable of labeling individual cells with distinct colors at a desired time point. Given that many GAL4 drivers have a pattern repeated in every half segment of the body, this could in more practical terms translate to multiple cases of tightly controlled single-cell labeling in a single sample. Combined with the fact that the expression of the two halves of the protein require that cells have *GAL4* activity, their light-inducible dimerization would make this otherwise highly robust DNA editing enzyme tamable. Thus, the split-*Cre* provides a means to control the onset of multicolor cell labeling in the *Drosophila* LOLLIbow system.

Multicolor assignment

The original Brainbow design uses three mutually exclusive variants of *lox*, which results in their use at near parity ratios (Livet et al., 2007). We chose Brainbow1.1, which encodes open reading frames of three fluorescent proteins after excision of a stochastically selected *lox* pair: RFP (mCherry), YFP (EYFP) and CFP (mCerulean) (Fig. 1A). These monomeric fluorescent proteins are characterized by brightness and photo-stability. We cloned this cassette into the *GAL4* responsive vector. The original polyadenylation site, *lox* sequences and plasma membrane-targeting palmitoylation tags were all preserved. When put together, this design ensured no expression of the cassette in the absence of *GAL4* and, when a *GAL4* driver is added, high expression levels in a defined set of cells. For example, combining the pan-neuronal *elav-GAL4* driver to the tricolor Brainbow cassette *UAS-brainbow* resulted in stochastic color assignments of neurons in the brain with RFP, YFP and CFP (Fig. 3). In *Drosophila*, for an unknown reason, the default state of this particular Brainbow construct in the absence of recombinase activity is co-expression of OFP and RFP. Nevertheless, all three colors that result from DNA editing, i.e. RFP (without OFP), YFP and CFP, are each clearly separable from the others. Having three colors may not suffice to distinguish neurons in the brain that are not only highly packed but also tend to display complex morphologies. However, expanding the color palette to include an unknown number of color choices might not necessarily

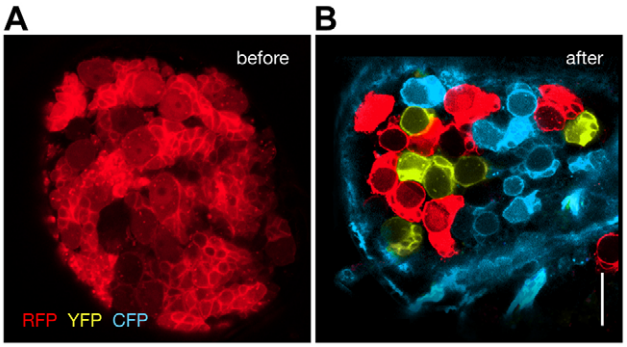

Fig. 3. Tricolor labeling. Larval brain labeled using *elav-GAL4* driver: (**A**) default expression (RFP) without recombinase activities; (**B**) tricolor labeling (RFP, YFP or CFP) with recombinase activities. Both OFP and RFP are expressed as default (see text). Scale bar: 10 μm.

make the situation better. Increasing the copy number of the Brainbow cassette from one to two, however, produced six distinct colors instead of three (Fig. 4). Knowing the exact copy number of the cassette within the genome permitted an unambiguous color separation. This could be useful, especially when tracing individual neurons with long axons that span across other neurons and tissues. Multicolor labeling of cells could also influence the experimental design. One goal of experiments using *GAL4* drivers is to isolate events that take place within cells of a discrete population. Here, the typical logic is as follows: the smaller the population size examined, the more straightforward becomes the interpretation of its data. With multicolor labeling, however, the strategy changes, i.e. use color separation and simultaneously watch events in a large number of cells, then seek impacts of interactions among cells of the same and/or different populations. For example, combining both *elav-GAL4* and GAL^{24B} drivers permitted simultaneous visualization of three motoneuron endings that are co-innervating a single muscle along with nearby tendon cells within a single animal (n=6 larvae, Fig. 5). In the larval neuromuscular system, the motoneurons of molecularly and functionally disparate properties control the entire set of skeletal muscles attached to corresponding tendon cells and surrounded by other cells of different functions. In order to characterize both genetic and activity-dependent mechanisms that contribute to the development of each neuromuscular synapse,

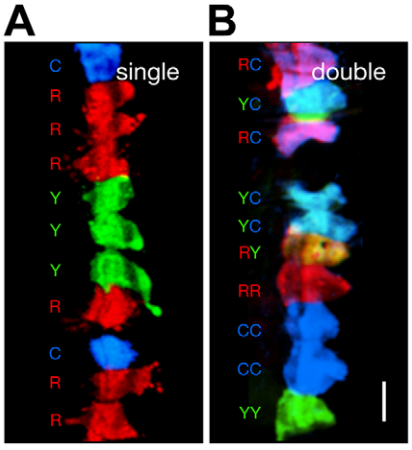

Fig. 4. Color variations. Tendon cells colored using the $GAL4^{24B}$ driver: (**A**) three colors with single copy of the Brainbow cassette; (**B**) six colors with double copies. Scale bar: 10 μm.

previous work depended on cell labeling techniques that reveal either all synapses indiscriminately or only small subsets of them. We propose that the 'image many, then analyze later' approach, which is possible using our system, could accommodate swift screens of cell-autonomous and non-autonomous events during this and other topics of research in developmental biology.

Morphological details

Morphogenesis of individual neurons depends upon interactions with neighboring neurons. One area that has rarely benefited from direct visualization *in vivo* is the interactions among neurons of the same molecular identities. Genotype-independent, stochastic multicolor labeling by Brainbow allows for many cells of the same type to be visualized individually with distinct colors (Livet et al., 2007). The fine details of individual neurons labeled with the stochastic Brainbow system can be visualized best by using epitope tags that permit nearly unlimited signal amplification (Livet et al., 2007; Hampel et al., 2011). Unfortunately, this method is not readily compatible with live imaging. An alternative, live imaging-compatible method would be to create, within each cell, a concentration gradient of fluorescence towards the plasma membrane. Both manually applied carbocyanine fluorescent dye DiI (Honig and Hume, 1986) and genetically delivered palmitoylated GFP (Moriyoshi et al., 1996) exemplify previous approaches that attain single-cell resolution without fixation of tissues. The effect of membrane-targeted fluorescence is, in fact, most striking when one visualizes neurons and non-neuronal cells known to extend very small and extremely fragile structures, such as filopodia, during development (Ritzenthaler et al., 2000; Kim et al., 2002). Because chemical and physical treatment are not required prior to imaging, data collection is accelerated, whereas issues of filopodia retraction and fluorescence loss are minimized. Interactions among neurons that posses equal competitive capabilities have been an area of intense research. Here, because of its compact size, the space in which intercellular interactions take place becomes small in *Drosophila*, enhancing the chance that individual neurons of equal molecular capacities can potentially touch one another. For example, bilateral neurons present on both sides of the brain extend their axonal and/or dendritic growth cones reciprocally. They would, therefore, encounter an identical molecular environment twice, i.e. before and after crossing the midline (Furrer et al., 2003). Peripheral sensory neurons that occur in reiterated patterns could also see their molecular environment repeated across the segmental border. Some such neurons are known to exhibit self-avoidance when establishing complex dendritic arborization patterns (Grueber et al., 2002; Grueber et al., 2003). *GAL4* drivers are, by nature, incapable of distinguishing individual cells among molecularly identical cells. As a result, simultaneous visualization of these and other cases of intercellular interactions among bilateral and segmental homolog neurons have previously relied on labor-intensive dye injection and/or computer-assisted tracing of individual neurons. LOLLIbow, however, was able to unveil the fine dendritic morphology of individual segmental homolog neurons in a live larva with distinct colors (n=4 third instar larvae, Fig. 6). Studies characterizing how various molecular signals sculpt neurons could benefit from the single-cell resolution and multicolor imaging of neurons that are molecularly identical and yet interact extensively with one another within an animal.

Live imaging

Understanding the mechanisms that regulate the morphological dynamics of cells is fundamental to developmental biology. In the

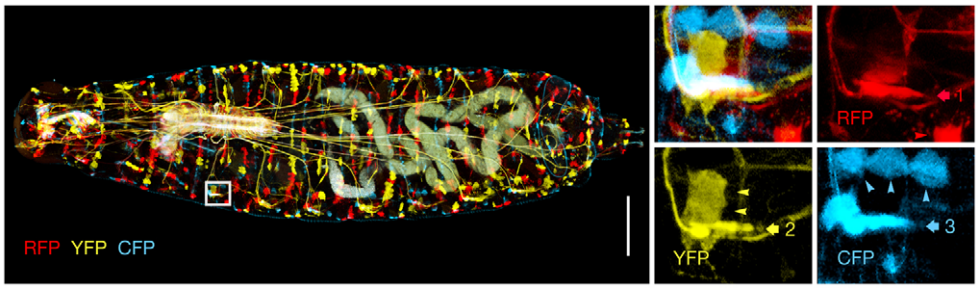

Fig. 5. Multiple drivers. Neurons and tendon cells in a larva using both *elav-GAL4* and *GAL4*^{24B} drivers. Box shows the area that is zoomed (right). Three motoneuron endings (arrows 1-3) co-innervating the same target muscle (unlabeled) near tendon cells (arrowheads). Scale bar: 100 μm.

past, persistent chromosomal staining and surgical ease had made the quail-chick chimera a popular model organism because it offers single-cell resolution (Le Douarin, 1980). Similarly, when studying the sequence of cellular events within intact animals using Brainbow-based multicolor imaging, a desirable feature would be stable color assignment. Depending on the orientation of their respective recognition sequences, both *Flp* and *Cre* recombinases can either excise or invert the Brainbow cassettes. One has, then, a choice of being able to label a cell with one permanent color or to re-assign different colors continuously to the same cell. We used the cassette that would permit only one excision in each cell. This allows for tracking, with certainty, how each cell divides, migrates or transforms over time. Several areas of study may be dramatically augmented using time-lapse analyses of cells labeled with permanently assigned colors. One is the area of synaptic plasticity. As shown in Fig. 5, the larval neuromuscular synapses are each multiply innervated (Hoang and Chiba, 2001). Their developmental plasticity and its physiological significance have been recognized in many studies (Budnik, 1996; Keshishian et al., 1996; Schuster et al., 1996). Here, an obvious advantage of live imaging would be that data could be collected at multiple time-points from the same samples. Zito et al. pioneered such a multiple time-point monitoring approach by labeling the membrane-enriched postsynaptic membrane with GFP (Zito et al., 1999). With LOLLIbow, one could expand analyses on the individual synapses (n=24 multiply-innervated neuromuscular synapses in four larvae, Fig. 7). The issue of how separate neuronal endings continue to enlarge yet maintain stereotyped morphology when adjusting their presynaptic machinery under continually varying environmental stimuli would be made tractable by unprecedented single-synapse resolution. Another area of study that could benefit from live imaging is analyses of animal behavior at single-cell resolution. Feeding, crawling and other innate behaviors are subjected to dynamic changes by variously imposed conditions or mutations. Using LOLLIbow, we were able to monitor the locomotion of newly hatched larvae at the level of individual tendon cells as they undergo complex patterns of force generation (n=3 first instar larvae; Fig. 8). Such *in situ* real-time cellular imaging could serve as criteria in phenotypic evaluation of many cell types. Perhaps the most unanticipated expanse of phenomena to benefit from single-cell resolution imaging could be found in the area of intercellular communication, namely in the form of direct exchange of their own molecules. In a variety of tissues, extremely fragile actin-based filopodia are known to contact neighboring cells. Such dynamic structures often appear postmitotically when the cells undergo concerted migration and/or differentiation. Membrane-targeted GFP has shown these transient yet direct means of intercellular communication, reaching as far as several cell diameters away from one another, not only among the neurons but also glial and muscle cells, as well as the epithelial cells (Ramírez-Weber and Kornberg,

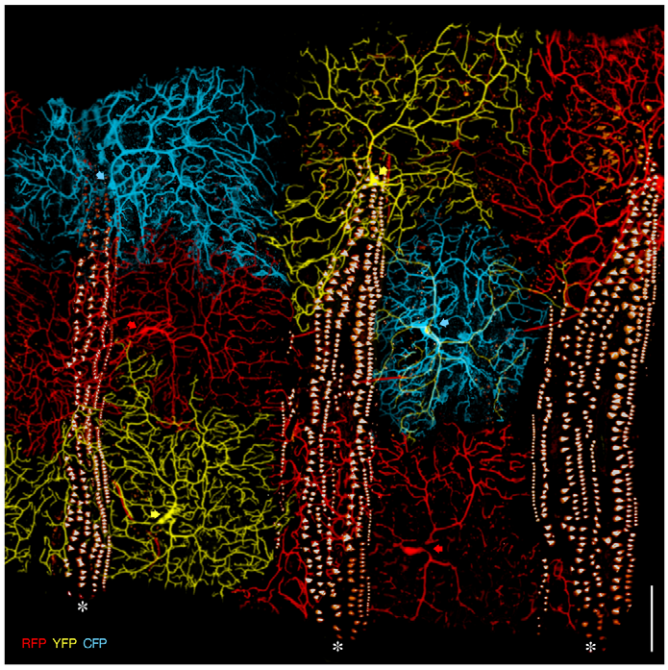

Fig. 6. Cellular morphology with single cell resolution. Multicolor labeling of PNS sensory neurons in the ventrolateral body wall of a larva using the *ppk'-GAL4* driver. The color assignment in these neurons (arrows) appears random. All fluorescent proteins are distributed throughout different cellular compartments within a given neuron. The image was acquired using three channels. Autofluorescence in denticles of the ventral cuticle delineates segment boundaries. Scale bar: 200 μm. Denticles in cuticle express broad spectrum autofluorescence, which appears nearly white on the image (asterisks).

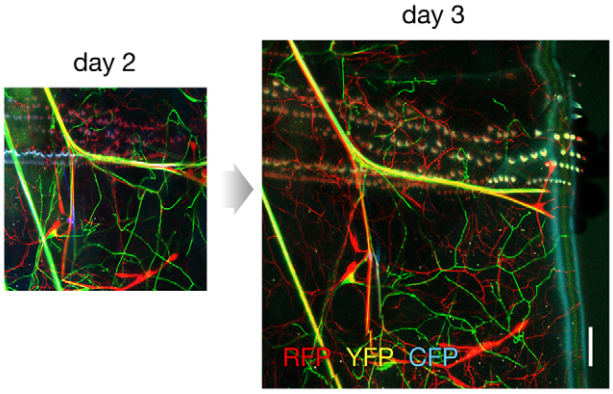

Fig. 7. Multiple time-point observation. Multiply innervated neuromuscular synapses undergo transformation into maturity, shown with single-synapse resolution using the *elav-GAL4* driver within a single larva at two time-points that are 24 hours apart. Scale bar: 100 μm.

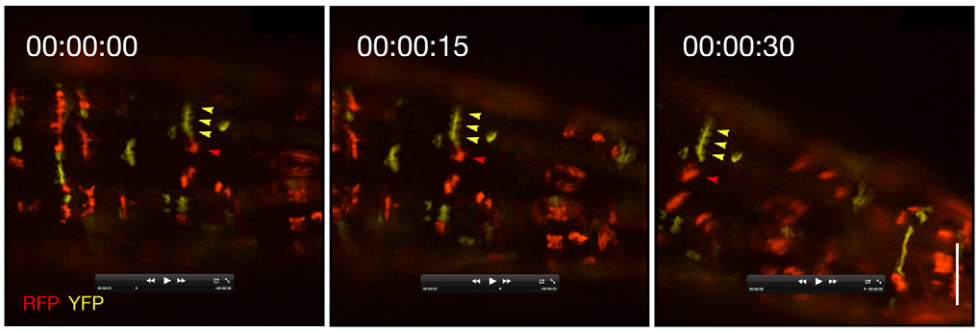

Fig. 8. Cellular dynamics during behavior. A crawling first instar larva exhibits rapid translocation and cell shape change of individual tendon cells (arrowheads), as visualized using the *GAL4*^{24B} driver. The total time-lapse movie duration is 30 seconds. Scale bar: 20 μm. (Supplementary material Movies 1 and 2.)

1999; Ritzenthaler et al., 2000; Vasenkova et al., 2006). In the isolated wing epithelia, GPI-anchored GFP, a way to target GFP to the outer leaf of the plasma membrane, has further revealed 'argosomes', which is taken as evidence for intercellular exchange of still undetermined molecules (Greco et al., 2001). The pupal case has often been considered off-limits to intact imaging because of its opacity. Between 24 and 48 hours after puparium formation (APF) the pupae are immobile, as they histolyze larval tissues and form the adult body. The combination of brightness and high expression levels of the fluorescent proteins facilitates direct image acquisition of superficial epithelia, such as the wing, during the pupal period. Furthermore, the multicolor labeling of our LOLLIbow system allows visualization of two classes of membrane-associated structures in intact epithelial cells that, by definition, must arise from their neighbor cells (n=27 movies in 20 pupae). First, the continually extending and retracting filopodia contact the surface of neighbors up to five cells away (Fig. 9A). Second, the 'argosomes' of varied diameters invade into the cytoplasm of neighbors (Fig. 9B). The first occurs predominantly in the basal side, whereas the second occurs frequently in the apical side of these cells. The mechanisms for each, especially how they form and what macromolecules they may contain, need further assessment. However, it is clear that the developing cells have an assortment of means to exchange their own molecules and that the multicolor stochastic cell labeling by LOLLIbow would be useful in gaining new insights.

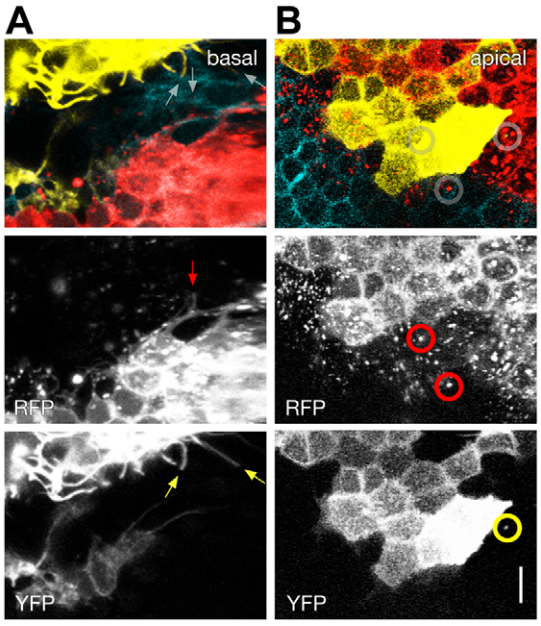

Fig. 9. Cellular dynamics during wing formation. (**A**) Filopodia (arrows) extend and retract actively to reach neighboring cells. (**B**) Argosomes (circles) diffuse around in the cytoplasm of neighboring cells. Scale bar: 10 μm. (Supplementary material Movies 1 and 2.)

Simple genetics

To facilitate studies that incorporate our new imaging system further, we established viable homozygous stocks. First, we combined the two transgenes encoding the complementary halves of split-*Cre* into a single chromosome: *UAS-CIBN::Cre-N,UAS-CRY2::Cre-C* (the 'split-*Cre*' stock). This stock would require both GAL4 and blue light to initiate *Cre* activities. It allows for a control over the cell type and its timing in which the DNA recombination occurs. Second, we combined the Brainbow transgene and the pan-neuronal *GAL4* driver in one fly line: *UAS-brainbow;elav-GAL4*, or the neuronal '*LOLLIbow*' stock. Because the *UAS-brainbow* transgene has been integrated near either end of the second chromosome, it will be straightforward to create additional 'LOLLIbow' stocks for various neuronal subpopulations or non-neuronal cell populations by recombining other *GAL4* drivers to *UAS-brainbow*. Thus, the morphogenesis of individual neurons or of other cell populations of choice in wild-type animals can now be examined with single-cell resolution in all the offspring from a single generation cross between 'split-*Cre*' and '*LOLLIbow*' stocks and following a brief pulse of blue light illumination given at a desired time point.

DISCUSSION

Five years ago, Livet et al. introduced their pioneering Brainbow system to the neurobiology and developmental biology communities (Livet et al., 2007). Today, one thing still missing in both fields, nevertheless, is vigorous application of this powerful technology in experiments performed with live whole animals. The reasons for this omission might have been part technical and part motivational in nature. We sought to push the methods for visualizing the dynamic cellular processes directly, with single-cell resolution, within intact organisms throughout their different stages of development.

All images in this paper were from live unfixed specimens of wild-type *Drosophila*. They were imaged using confocal microscopy at various developmental stages. A laser-scanning fluorescent microscope equipped with photomultiplier tubes was used to collected most images, while one movie that captured fast cellular behavior was acquired using a CCD equipped spinning disc confocal microscope. However, any conventional confocal system capable of spectrally separating the signals from the fluorescent proteins used in our system should be able to provide similar results (see Materials and methods). To preserve fluorescence of cell labels as well as the health of the living samples, a minimal number of detection channels and illumination time were employed in our

visualization. Neurons in the CNS and PNS, muscle cells, as well as the tendon cells in epidermis were examined live at embryonic, larval and pupal stages. The timing of their color assignment varied so that either the entire lineage or each postmitotic cell of a given lineage inherited a distinct color. Time-lapse movies captured fast cellular events during locomotion, as well as slow cellular events during metamorphosis. Most importantly, we encountered no visible sign of abnormality in development of the samples either during or following data collection.

Drosophila offers, in addition to its advanced genetics, a body that is largely transparent yet small. During much of its development, its vital organs, including the nervous system, remain within the penetration distance of conventional fluorescent microscopes. In addition, its rapid overall development involves both the embryonic and pupal periods, which are notable for their outward quiescence (i.e. they do not need to be fed) while simultaneously exhibiting spectacular cellular rearrangements internally. Therefore, it is an ideal choice for imaging cells *in toto*, i.e. within an intact animal. When designing experiments relevant in neurobiology and/or developmental biology, LOLLIbow offers several noteworthy features. First, our system has the potential to help explore the central issue in neurobiology: that neurons are the most highly connected cells found in animals. It is widely believed that much of what makes the brain so unique among a variety of tissues found in an animal comes from the precise connectivity of its neurons. However, the synapses and the circuitries they create are not only very small, but continue to be modified throughout the life of an individual animal. If the dynamic morphologies of many neurons were simultaneously accessible to live *in situ* imaging, this would provide a powerful research tool. Because all fluorescent proteins in our system, after *Cre*-mediated DNA recombination, are each targeted to the plasma membrane via a palmitoylation mechanism, their fluorescence would be concentrated preferentially at the membrane-rich structures within each cell. Therefore, one would be able to visualize such delicate structural details as secondary and tertiarily dendritic branches of individual neurons *in vivo* (for example, Figs 7, 9) or motoneuron endings co-innervating the same synaptic target muscle (for example, Figs 6, 10). Second, LOLLIbow is capable of addressing recurrent themes in developmental biology. For example, isolation of cell-autonomous functions in variously manipulated cells is a routine cell biological issue. Cell type-independent multicolor assignment by split-*Cre* recombinase could substantially increase the number of cells being analyzed in a given experiment. Equally important is inducibility, allowing one to assign colors to individual cells at any desired time point during their development. This could become very handy when one wishes to visualize explicitly, for example, all cells with one color that are derived from a single stem cell or, alternatively, assign separate colors to each of its offspring cells. Furthermore, because individual cells carry stable and spectrally separable fluorescent proteins, tracking a given population of cells would be possible as they migrate through other tissues and transform their own morphologies. Third, our system is modular. For example, the inducible split-*Cre* could also combine with immunology-ready dBrainbow. In addition, because our system relies neither on heat shock nor on *Flp* recombinase, it could be easily combined with experiments that use thermosensitive *GAL80* and/or *Flp* recombinase, such as MARCM, for additional genetic manipulations. In fact, one could use split-*Cre* to label a specific cell population and then turn, for example, to antibody staining for further visualization using electron or super resolution microscopy. Defects in neuronal morphology underlie many human neurodevelopmental disorders such as autism and mental retardation (Kaufmann and Moser, 2000). Consequently, the process of synaptogenesis, axon pathfinding and dendritic morphogenesis has been intensely studied in *Drosophila*. The LOLLIbow system would be particularly well-suited for analysis on, for example, dendritic tiling of receptive fields by neighboring neurons (Corty et al., 2009), as well as dendrite-substrate interactions that are thought to mediate dendritic self-avoidance (Kim et al., 2012) and the establishment and maintenance of dendritic fields (Parrish et al., 2009). Finally, and perhaps most significantly, LOLLIbow is compatible with live imaging. With the ability to see through the whole organism, experimental biology will have exciting opportunities to redefine its resolution down to the level of individual cells.

Are there features that could be improved in our system? First, the tricolor labels are uneven in their brightness. Replacing the most difficult to detect CFP with a reportedly twofold brighter mTFP1 and/or tandemizing the monomer seems a viable option. Second, the perdurance of the default fluorescent proteins is longer than ideal. It typically is close to 24 hours before the newly produced multicolor fluorescent proteins become readily visible against this background. Attaching a PEST sequence to the default fluorescent proteins could minimize this problem. Third, the recombination efficiency of the split-*Cre* is most probably not yet optimal. To resolve this, we could redesign the molecular structure of the *Cre* halves to achieve a higher affinity and stability as dimer. One thing that can be attempted immediately, however, is to deliver the blue light as a focused laser beam so that one would gain the control over not only the timing but also the position of the multicolor labeling within a given animal.

In conclusion, the new Brainbow system for *Drosophila* described here is anticipated to facilitate examination of dynamic morphological events that are exquisitely coordinated by neuronal and other defined populations of cells within living model animals. By complementing existing experimental tools, its use will probably yield vital insights into the development of multicellular organisms under both normal and experimental conditions.

Acknowledgements
We thank Daichi Kamiyama, Gavriil Tsechpenakis, Nima Sharifai, Sophie Deng, Jeff Peng and Rod Murphey for critical reading of manuscript, and Sarah Marmol and Jeff Lowell for technical assistance.

Funding
This work was funded by the National Institutes of Health (NIH) [NS06948 and MH079432 to A.C.]. Deposited in PMC for release after 12 months.

Competing interests statement
The authors declare no competing financial interests.

Supplementary material
Supplementary material available online at
http://dev.biologists.org/lookup/suppl/doi:10.1242/dev.088930/-/DC1

References
Budnik, V. (1996). Synapse maturation and structural plasticity at Drosophila neuromuscular junctions. *Curr. Opin. Neurobiol.* **6**, 858-867.
Corty, M. M., Matthews, B. J. and Grueber, W. B. (2009). Molecules and mechanisms of dendrite development in Drosophila. *Development* **136**, 1049-1061.
Förster, D. and Luschnig, S. (2012). Src42A-dependent polarized cell shape changes mediate epithelial tube elongation in Drosophila. *Nat. Cell Biol.* **14**, 526-534.
Furrer, M. P., Kim, S., Wolf, B. and Chiba, A. (2003). Robo and Frazzled/DCC mediate dendritic guidance at the CNS midline. *Nat. Neurosci.* **6**, 223-230.
Greco, V., Hannus, M. and Eaton, S. (2001). Argosomes: a potential vehicle for the spread of morphogens through epithelia. *Cell* **106**, 633-645.
Grueber, W. B., Jan, L. Y. and Jan, Y. N. (2002). Tiling of the Drosophila epidermis by multidendritic sensory neurons. *Development* **129**, 2867-2878.

Grueber, W. B., Ye, B., Moore, A. W., Jan, L. Y. and Jan, Y. N. (2003). Dendrites of distinct classes of Drosophila sensory neurons show different capacities for homotypic repulsion. *Curr. Biol.* **13**, 618-626.
Hadjieconomou, D., Rotkopf, S., Alexandre, C., Bell, D. M., Dickson, B. J. and Salecker, I. (2011). Flybow: genetic multicolor cell labeling for neural circuit analysis in Drosophila melanogaster. *Nat. Methods* **8**, 260-266.
Hampel, S., Chung, P., McKellar, C. E., Hall, D., Looger, L. L. and Simpson, J. H. (2011). Drosophila Brainbow: a recombinase-based fluorescence labeling technique to subdivide neural expression patterns. *Nat. Methods* **8**, 253-259.
Heidmann, D. and Lehner, C. F. (2001). Reduction of Cre recombinase toxicity in proliferating Drosophila cells by estrogen-dependent activity regulation. *Dev. Genes Evol.* **211**, 458-465.
Hoang, B. and Chiba, A. (2001). Single-cell analysis of Drosophila larval neuromuscular synapses. *Dev. Biol.* **229**, 55-70.
Honig, M. G. and Hume, R. I. (1986). Fluorescent carbocyanine dyes allow living neurons of identified origin to be studied in long-term cultures. *J. Cell Biol.* **103**, 171-187.
Kaufmann, W. E. and Moser, H. W. (2000). Dendritic anomalies in disorders associated with mental retardation. *Cereb. Cortex* **10**, 981-991.
Kennedy, M. J., Hughes, R. M., Peteya, L. A., Schwartz, J. W., Ehlers, M. D. and Tucker, C. L. (2010). Rapid blue-light-mediated induction of protein interactions in living cells. *Nat. Methods* **7**, 973-975.
Keshishian, H., Broadie, K., Chiba, A. and Bate, M. (1996). The drosophila neuromuscular junction: a model system for studying synaptic development and function. *Annu. Rev. Neurosci.* **19**, 545-575.
Kim, M. D., Kolodziej, P. and Chiba, A. (2002). Growth cone pathfinding and filopodial dynamics are mediated separately by Cdc42 activation. *J. Neurosci.* **22**, 1794-1806.
Kim, M. E., Shrestha, B. R., Blazeski, R., Mason, C. A. and Grueber, W. B. (2012). Integrins establish dendrite-substrate relationships that promote dendritic self-avoidance and patterning in drosophila sensory neurons. *Neuron* **73**, 79-91.
Le Douarin, N. M. (1980). The ontogeny of the neural crest in avian embryo chimaeras. *Nature* **286**, 663-669.
Lee, T. and Luo, L. (1999). Mosaic analysis with a repressible cell marker for studies of gene function in neuronal morphogenesis. *Neuron* **22**, 451-461.
Livet, J., Weissman, T. A., Kang, H., Draft, R. W., Lu, J., Bennis, R. A., Sanes, J. R. and Lichtman, J. W. (2007). Transgenic strategies for combinatorial expression of fluorescent proteins in the nervous system. *Nature* **450**, 56-62.
Luk'ianov, K. A., Gurskaia, N. G., Bogdanova, E. A. and Luk'ianov, S. A. (1999). [Selective suppression of polymerase chain reaction]. *Bioorg. Khim.* **25**, 163-170.
Lukyanov, K. A., Matz, M. V., Bogdanova, E. A., Gurskaya, N. G. and Lukyanov, S. A. (1996). Molecule by molecule PCR amplification of complex DNA mixtures for direct sequencing: an approach to in vitro cloning. *Nucleic Acids Res.* **24**, 2194-2195.
Moriyoshi, K., Richards, L. J., Akazawa, C., O'Leary, D. D. and Nakanishi, S. (1996). Labeling neural cells using adenoviral gene transfer of membrane-targeted GFP. *Neuron* **16**, 255-260.
Parrish, J. Z., Xu, P., Kim, C. C., Jan, L. Y. and Jan, Y. N. (2009). The microRNA bantam functions in epithelial cells to regulate scaling growth of dendrite arbors in drosophila sensory neurons. *Neuron* **63**, 788-802.
Ramírez-Weber, F. A. and Kornberg, T. B. (1999). Cytonemes: cellular processes that project to the principal signaling center in Drosophila imaginal discs. *Cell* **97**, 599-607.
Ritzenthaler, S., Suzuki, E. and Chiba, A. (2000). Postsynaptic filopodia in muscle cells interact with innervating motoneuron axons. *Nat. Neurosci.* **3**, 1012-1017.
Schuster, C. M., Davis, G. W., Fetter, R. D. and Goodman, C. S. (1996). Genetic dissection of structural and functional components of synaptic plasticity. II. Fasciclin II controls presynaptic structural plasticity. *Neuron* **17**, 655-667.
Siegal, M. L. and Hartl, D. L. (1996). Transgene Coplacement and high efficiency site-specific recombination with the Cre/loxP system in Drosophila. *Genetics* **144**, 715-726.
Vasenkova, I., Luginbuhl, D. and Chiba, A. (2006). Gliopodia extend the range of direct glia-neuron communication during the CNS development in Drosophila. *Mol. Cell. Neurosci.* **31**, 123-130.
Volk, T. (1999). Singling out Drosophila tendon cells: a dialogue between two distinct cell types. *Trends Genet.* **15**, 448-453.
Zito, K., Parnas, D., Fetter, R. D., Isacoff, E. Y. and Goodman, C. S. (1999). Watching a synapse grow: noninvasive confocal imaging of synaptic growth in Drosophila. *Neuron* **22**, 719-729.